

Hybrid Thinking in Vision-Language-Action Models

Anonymous Author(s)

Affiliation

Address

email

1 **Abstract:** Using Large Language Models to produce intermediate thoughts before
2 providing a final answer has been a successful recipe for solving increasingly
3 complex tasks with reduced human supervision. In robotics, similar embodied rea-
4 soning strategies have also been shown to lead to improved performance. However,
5 as these techniques increase the length of the model’s outputs to include reasoning
6 traces, the inference time is negatively affected. Delaying an agent’s actions in
7 real-world executions, as in robotic manipulation settings, can be particularly prob-
8 lematic, as the agent needs to perform long sequences of actions before solving a
9 task. In this work, we establish a Hybrid Thinking (HyT) framework for training
10 Vision-Language-Action (VLA) models. Agents can learn both to directly answer
11 with actions (fast mode) or to spend more time thinking (slow mode). We show that,
12 even when generating no thoughts, in fast mode, the agent performance benefits
13 from training on the reasonings that leads to successful actions. Our agent demon-
14 strates improved performance at lower inference costs, and greater scalability with
15 larger datasets across a set of different robotic manipulation tasks. Additionally,
16 hybrid thinking allows humans to interpret the agents’ intentions and intervene on
17 them to prevent failures for complex tasks’ execution.

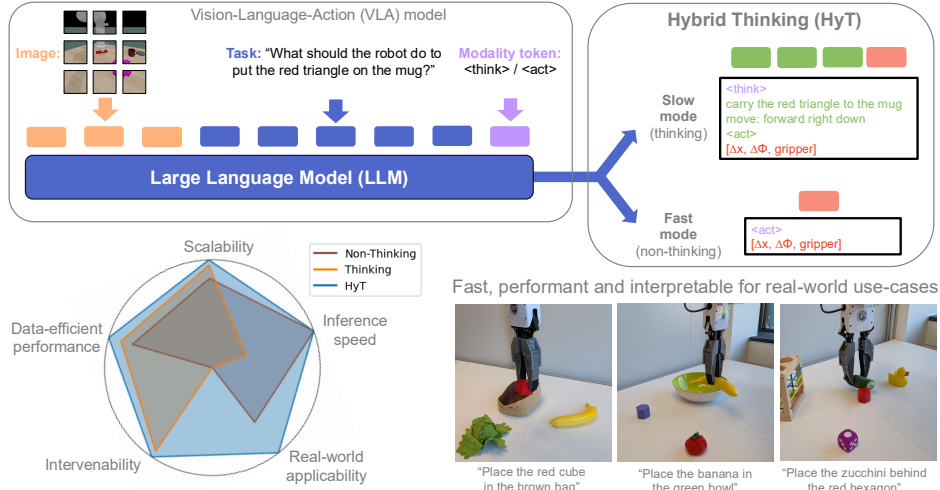


Figure 1: **Hybrid Thinking VLAs.** The hybrid thinking framework enables vision-language-action models to work either in fast, acting, mode or thoughtful, slow, execution. In fast mode, the agent retains high performance, at high inference speed, facilitating deployment in real-world platforms. In slow mode, the model grants high interpretability and the possibility of intervening on its thoughts, to change the predicted course of actions. Further details about the Figure are provided in the Appendix.

18 1 Introduction

19 Despite recent advances in robotics, truly generalist robot policies have long been elusive. Thanks to
20 the joint efforts of collecting large-scale robot data [1] and making large Vision Language Models

21 (VLM) open-source [2, 3], we have entered a new era in robotics foundation models. By fine-tuning
22 VLMs on robotic datasets containing actions, we can create Vision-Language-Action models (VLAs)
23 [4, 5, 6]. These large policy models are trained end-to-end to take language instructions and raw
24 camera images as inputs, and output low-level actions for the robot to perform.

25 VLAs possess several advantages over previous work, such as multimodal prompting of the agent
26 and the availability of knowledge from the base pre-trained VLM. However, generalization to out-of-
27 distribution (OOD) settings, e.g., task configurations not available in the robotics training dataset,
28 remains challenging. Indeed, the knowledge of the agent is vast about general concepts, but remains
29 limited in the robotics settings, where the data distribution is often narrow.

30 In order to further unleash the capabilities of VLAs, recent works have explored adding Chain-of-
31 Thought (CoT) reasoning [7] while training VLAs [8]. This class of *thinking VLA* models learns
32 to output useful information about the given task in language form, before generating the actions
33 to execute. This not only has shown to improve performance, but it also allows humans to more
34 easily interpret the agent’s intentions and potentially intervene on them, i.e. manipulating the agent’s
35 thoughts, before action generation. However, due to the large amount of reasoning outputs generated
36 before actions, the inference time of these models is significantly higher.

37 Similarly to thinking VLAs, *hierarchical VLA* methods [9, 10] aim to improve performance by
38 leveraging a two-level system. A high-level VLM processes the instructions and the information from
39 the environment and provides an actionable plan. A low-level VLA policy receives the higher-level
40 plan as an instruction and generates robotic actions to execute accordingly. This class of VLAs offers
41 similar benefits and drawbacks as thinking VLAs: they can improve performance and allow humans
42 to read and/or manipulate the agent’s intentions, but they come with an even higher inference cost.

43 The human cognition process from observation to action has been hypothesized to leverage the
44 interaction of two systems [11]. The fast and intuitive *System I* handles most daily tasks, taking
45 control in contexts that our brain judges as unchallenging. The slow and deliberate *System II* is
46 activated when decisions require additional computation, such as comparing options or processing
47 complex information. The tendency of the brain is to delegate decisions to System II only when it’s
48 really necessary, to save energy and time. Humans can improve the capabilities of their System I,
49 developing a skilled intuition [12] to solve complex but familiar tasks effortlessly.

50 We hypothesize that VLA models can similarly develop more skilled intuition. Learning from the
51 CoT reasoning traces, a model should be able to internalize knowledge about environments and tasks.
52 Then, during test-time, the model should more easily recognize patterns, even without generating any
53 thoughts. With this hypothesis in mind, we develop a **hybrid thinking** (HyT) framework, where the
54 agent learns to operate in different modes, thinking and non-thinking ones, within a single model.

55 Hybrid thinking can be effectively implemented by teaching the model to predict a variety of outputs,
56 which are sampled with different probabilities during training. During test-time, the model can operate
57 in different modes: primarily a fast mode and a slow mode. The fast mode improves performance over
58 standard VLAs, while having no higher inference costs. The slow mode could be employed in critical
59 settings, where interpreting the agent’s intentions or allowing interventions from humans could be
60 useful. In addition to investigating the hybrid thinking framework, we aim to address a fundamental
61 question regarding VLA models: *What is the contribution of reasoning and CoT techniques to their
62 performance?*

63 **Our contributions are:**

- 64 • We establish the hybrid thinking (HyT) framework for vision-language-action (VLAs)
65 models. We present an implementation of HyT which has a Fast and a Slow mode, enabling
66 both fast action inference and rational thinking when necessary, within the same model.
- 67 • We empirically validate our approach, highlighting its data-efficiency, scalability and inter-
68 venability across a large quantity of simulated experiments.
- 69 • We perform a real-world experiment on a UFactory xArm 6 that showcases the applicability
70 of the approach in real robotics settings.

71 **2 Related Work**

72 **Vision-Language-Action models.** Open-source efforts in the robotics field, such as the Open X-
73 Embodiment dataset [1], have fueled progress in the development of large VLAs [4, 13, 14, 15, 16].
74 Recent works have also explored hierarchical VLA architectures [9, 10], showing they can be
75 beneficial for solving open-ended and long-horizon tasks.

76 **Chain-of-Thought and reasoning.** Generating a chain of thought has shown improved performance
77 in LLMs solving complex reasoning tasks [17]. Recently, reasoning has shown notable success using
78 RL with verifiable rewards, coupled with Supervised Finetuning (SFT) on example reasoning traces
79 [18, 19]. CoT techniques specifically for VLMs [20] and VLAs have also been researched [8, 21].
80 In particular, ECoT [8] shows that embodied thoughts can greatly improve the agent’s predictions
81 in robotics, despite the higher inference costs. Our work grounds on their findings and proposes a
82 method that accomplishes both strong performance and fast inference.

83 **Hybrid reasoning.** Recent works have attempted to distill slow thinking capabilities into faster
84 models [22, 23]. Closely related to our method is DualFormer [24], proposes to train a language
85 model by systematically dropping out reasoning traces. In robotics domain, RFST [25] proposes a
86 hierarchical setup that uses a discriminator to decide whether to switch to the fast or slow system,
87 with the respective model of the chosen mode being then used as the policy. Our work, instead,
88 focuses on providing a single system that is capable of both thinking and acting.

89 **3 Method**

90 **3.1 Formal definitions**

91 Vision-Language Action models are multimodal policies generally trained with imitation learning.
92 A VLA processes language inputs through a Transformer-based LLM architecture [26, 27, 28].
93 Language is first "tokenized" into language tokens that are then processed by the LLM. Similarly,
94 VLAs can process visual inputs through a vision encoder, e.g., a vision transformer [29], that
95 transforms image patches into visual tokens, which are then processed by the LLM.

96 Given a language description of a task ℓ , the goal of the VLA policy is to solve the task in a given
97 environment. The policy observes the environment through images x , generally captured by a camera
98 in the environment. The policy interacts with the environment using actions a . Through imitation
99 learning, the policy’s objective is to learn, at each discrete timestep, the distribution $p(a_t|x_t, \ell)$ that
100 solves the given task, which is empirically observed from a dataset of demonstrations. In this work,
101 we assume that actions are mapped to tokens in the LLM’s vocabulary, through a discretization
102 scheme that assigns continuous values to one of the 256 bins [4]. This enables the LLM to predict
103 action tokens in the same vocabulary space as language tokens. A VLA policy can be defined as:

$$\text{VLA: } p(a_t|x_t, \ell) = p_\theta(a_t|x_t, \ell).$$

104 In addition to predicting actions, thinking VLAs [8] are also capable to reason about the task and
105 the environment. These reasonings are expressed as thoughts τ in language form, predicted by the
106 model. Generally, thoughts include information about the overall plan of action, the current subtask
107 to execute, the location of objects in the image, or the direction of the agent’s ongoing motion [8]. A
108 thinking VLA policy can be defined as:

$$\text{Thinking VLA: } p(a_t, \tau_t|x_t, \ell) = p_\theta(a_t|x_t, \ell, \tau_t)p_\theta(\tau_t|x_t, \ell).$$

109 Thinking VLAs learn a single set of parameters θ to predict both actions and thoughts. Hierarchical
110 VLAs [9, 10] use a two-level hierarchy of models, where one model is to provide an actionable plan
111 for solving the task, while the second model should execute the plan. As shown in [9], predicting the
112 current plan to solve the task can be as simple as predicting the current subtask and motion primitives.
113 Thus, we treat high-level plans and thoughts interchangeably in this work. A hierarchical VLA policy
114 can be defined as:

$$\text{Hierarchical VLA: } p(a_t, \tau_t|x_t, \ell) = p_{\theta_\ell}(a_t|x_t, \tau_t)p_{\theta_h}(\tau_t|x_t, \ell),$$

115 where θ_h denotes the parameters of the “high-level” model, θ_ℓ denotes the parameters of the “low-
116 level” model, and the models’ hierarchy enforces $(a_t \perp\!\!\!\perp \ell | \tau_t)$, i.e. the conditional independence
117 between actions and language instructions, given thoughts.

118 **3.2 Hybrid Thinking**

119 Thinking and hierarchical VLAs have demonstrated improved performance over a standard VLA
120 [9, 10, 8]. However, generating thoughts comes at a high inference cost, as they generally consist of
121 significantly more tokens than their action counterpart. This can significantly slow down the agent’s
122 action execution in the environment.

123 We hypothesize that the primary benefits of these models arise not from the generated thoughts
124 themselves, but from the knowledge learned by the model through thought prediction. This suggests
125 that the model refines its intuitive capabilities by internalizing the patterns present in the thoughts,
126 akin to the development of intuitive expertise [12]. Under this hypothesis, after a learning process
127 that is similar to those of thinking and hierarchical models, a VLA should be able to predict actions
128 with higher accuracy, with or without the thoughts as an input.

129 To address the need for agents capable of producing multiple probability distributions within a single
130 model, we introduce a new thinking strategy, *Hybrid Thinking* (HyT), designed to integrate structured
131 reasoning with flexible policy learning.

132 **Definition 3.1 (Hybrid Thinking)** *Given a task description ℓ and the current environment observation x_t , the conditional distribution over actions a_t can be expressed as:*

$$p(a_t|x_t, \ell) = \sum_i \sum_j p(a_t, \tau^i, m^j | x_t, \ell) = \sum_i \sum_j p(a_t, \tau^i | x_t, \ell, m^j) p(m^j), \quad (1)$$

134 by marginalizing out thoughts τ and a “modality” variable m .

135 The hybrid thinking formulation enables to describe a VLA model that learns different thoughts and
136 conditional action distributions depending on a modality variable.

137 **3.3 Training VLAs with Hybrid Thinking**

138 Leveraging the insights from other VLA models, we can use the hybrid thinking framework to
139 conditionally learn three distributions:

$$p(a_t|x_t, \ell) = \underbrace{p(a_t|x_t, \ell, m^a)p(m^a)}_{\text{Act}} + \underbrace{p(a_t|x_t, \ell, \tau_t)p(\tau_t|x_t, \ell, m^\tau)p(m^\tau)}_{\text{Think}} + \underbrace{p(a_t|x_t, \tau_t, m^f)p(m^f)}_{\text{Follow}}. \quad (2)$$

140 The utility of each distribution is defined as follows:

- 141 • **“Act” action distribution:** following from $p(\tau = \emptyset | m^a) = 1$, is defined to predict only actions.
142 This modality enables fast inference time, by predicting no thoughts.
- 143 • **“Think” joint distribution:** predicts thoughts and actions. This modality fosters the model to learn
144 the thoughts distribution and to condition action predictions both on the task and the thoughts.
- 145 • **“Follow” action distribution:** follows from $p(a_t|x_t, \tau_t, m^f) = p(a_t|x_t, \ell, \tau_t, m^f)$ and
146 $p(\tau = \emptyset | m^f) = 1$. This modality assumes that thoughts are provided to the policy and it en-
147 courages the model to follow them closely for action prediction, as they replace the language task
148 in the inputs.

149 We can then assign the probabilities for different realizations of m to a set of values, which allows us
150 to define a stable VLA formulation:

$$p(a_t|x_t, \ell) = w_a \cdot p_\theta(a_t|x_t, \ell, m^a) + w_\tau \cdot p_\theta(a_t|x_t, \ell, \tau_t)p(\tau_t|x_t, \ell, m^\tau) + w_f \cdot p_\theta(a_t|x_t, \tau_t, m^f), \quad (3)$$

151 where $w_a = p(m^a)$, $w_f = p(m^f)$ and $w_\tau = p(m^\tau)$ are the probabilities of a modality variable
152 following a categorical distribution and θ denotes the parameters of the model.

153 In order to train a HyT VLA, we define the weights w_a, w_τ, w_f as the probabilities of sampling the
154 corresponding inputs and outputs for the model during training. This way, at each batch sampled
155 during training, the model receives modality tokens, actions and thoughts, with probabilities that
156 are defined by the coefficients. The model inputs and outputs are formed as in Equation 3. Then,
157 the model's parameters are trained to minimize the cross-entropy loss on future tokens predicted
158 autoregressively with causal mask attention [26].

159 During inference, we can prompt the model with different modality sets of tokens. These are defined
160 as $m^a = \langle \text{act} \rangle$, $m^\tau = \langle \text{think} \rangle$ and $m^f = \emptyset$ ¹). Depending on the modality token received, the model
161 is able to provide the corresponding modality's outputs, as also depicted in Figure 1.

162 **Intuitive explanation of the “follow” distribution.** Ideally, the model should be able to follow the
163 information in the thoughts by learning the joint distribution from the “Think” modality. However,
164 as the model is concurrently trained to predict actions, independently of the thoughts, the model
165 could tend to ignore the thoughts. Humans may want to possibly manipulate the agent’s thoughts for
166 correcting its action predictions. Thus, it is important that changes in the thoughts have a noticeable
167 impact on the action prediction, and the “Follow” distribution encourages such tendency.

168 4 Experiments

169 We evaluate the proposed HyT VLA in a series of simulated experiments, which we use to reliably
170 assess the model's capabilities, and on a set of real-world tasks, which demonstrates the practical
171 applicability of the approach.

172 General setup

173 Across all models, the task description is provided in the same format, i.e. “*What should the robot
174 do to {task}?*”. Image inputs are 224×224 RGB images from a camera pointing at the robot's
175 workspace. The action space is 7-dimensional and defined as: $[\Delta x, \Delta \phi, \text{gripper}]$. The end-effector
176 position x and orientation ϕ are controlled in delta space, while the gripper pose is in absolute value.

177 For all the thoughts, we adopt the same format, which includes the current subtask and, for the
178 *moving* subtask, the main direction of the movement. This simple definition has proven effective
179 across different models in early stages of our analysis and also in related work [9]. More elaborate
180 thoughts could include object bounding boxes or justification of the agent's actions [8], but we
181 decided against this as it would also significantly increase the amount of resources needed for training
182 and the inference time for thinking models due to the increasing number of generated tokens.

183 For HyT, during training, the different modality tokens are sampled with equal probabilities, i.e.
184 $p = 0.33$. During inference, we use the denomination “Fast mode” to refer to the “Act” modality
185 during inference and “Slow mode” to refer to the “Think” modality. The mode is set by forcing
186 the first tokens of the agent's output to be the set of tokens corresponding to $m^a = \langle \text{act} \rangle$
187 or $m^\tau = \langle \text{think} \rangle$. There is no switch between the two modalities within the same episode:
188 we evaluate them differently, to test the different agent capabilities. Designing an orchestration
189 mechanism that allows switching the two modalities for adaptive reasoning within the same episode
190 is left for future work.

191 The training for all experiments and approaches is done using PyTorch DDP [30] on 4 A100 GPUs.
192 Inference requires less than 20GB VRAM and is performed on a multi-instance A100 for simulated
193 environments and on an RTX A5000 for real-world experiments.

194 4.1 Simulated Experiments

195 For the simulated experiments, we employ the ClevrSkills benchmark [31], which is based on the
196 ManiSkill2 manipulation environments [32]. This environment includes an oracle solver to collect

¹For the follow modality defined by m^f there's no modality tokens, but the model can still discriminate it from the other modalities as the follow modality enforces no task description.

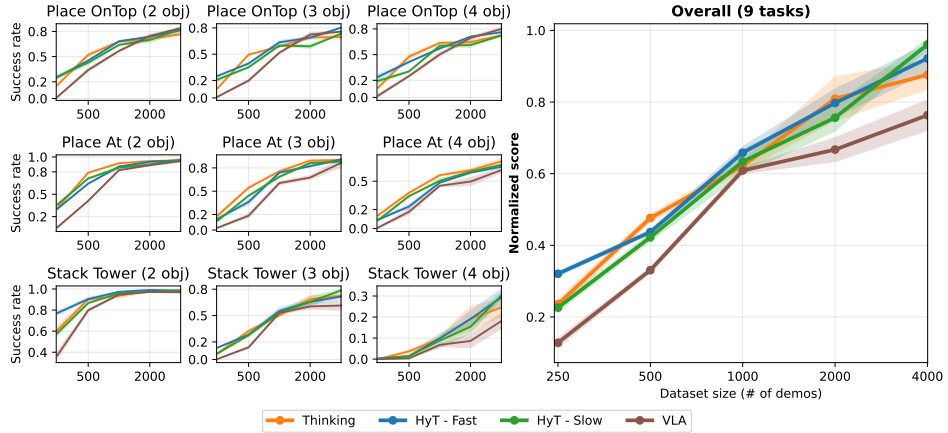


Figure 2: **Performance scalability.** On the left, success rate per task for three task groups (one per row). For each task group, agents are trained on a dataset containing a number of demonstrations from that task group that is showed on the x-axis (which uses a log scale). Then, the agent is evaluated on the three tasks of the group, averaging performance over 100 episodes \times 3 checkpoints. On the right, normalized scores averaged across all the tasks and evaluations.

197 demonstrations, and reasoning traces from the oracle, which we can use to discriminate subtasks
 198 and extract thoughts. ClevrSkills also adopts a vacuum gripper and mostly uses simple shapes and
 199 objects, avoiding the challenges of manipulating complex objects, which may require more complex
 200 action prediction heads [33, 34].

201 Using the oracle, we collect a diverse set of training data which spans three task groups: *Place At*,
 202 evaluating the agent’s spatial understanding, *Place OnTop*, evaluating the agent’s understanding of
 203 interactions between objects, and *Stack Tower*, evaluating longer-horizon capabilities. Further details
 204 about the tasks and the datasets’ definition are provided in Appendix.

205 For all approaches, we start from the PaliGemma-2 VLM model with 3B parameters [2], which is
 206 based on the Gemma-2 LLM [28] and on the SigLIP vision encoder [35]. We perform full-finetuning
 207 of the model with a batch size of 8 and a learning rate of $2e-5$, using the Adam optimizer [36]. For
 208 the hierarchical VLA approaches, we train two distinct PaliGemma-2 models.

209 During evaluation, we run the agent in the environment for 100 evaluation episodes. At inference
 210 time, we found that non-thinking VLA output actions at around ~ 3 Hz, while running 4 models in
 211 parallel on A100 GPUs. Thinking models are $2.5\text{-}3\times$ slower. Hierarchical models are $\sim 4\times$ slower.

212 Data-scaling experiments

213 The ability to scale with data and compute is a crucial criterion when aiming to build general purpose
 214 agents [37]. With this experiment, we aim to verify the hypothesis that HyT VLA can develop
 215 intuitive thinking through the hybrid training strategy. If the hypothesis is correct, we expect: i) that
 216 HyT VLA in Slow mode performs as well as thinking or hierarchical VLA models, ii) that HyT VLA
 217 in Fast mode performance is better than a standard VLA.

218 In this section, we also verify scaling properties of HyT. We adopt a set of three datasets, one for each
 219 task group, and train models at different data scales, up to 4000 demos per task. We show results in
 220 Figure 2. The normalized scores on the right are obtained by dividing each task’s success rates by the
 221 highest success rate we obtained in all experiments, such that the highest performance obtained by at
 222 least one of the approaches corresponds to 1 for all tasks (see Appendix for details). Normalizing
 223 scores this way is a common strategy when comparing agents evaluated on multiple tasks that have
 224 different performance scales [38, 39, 40].

225 Overall, we observe that the performance of all approaches scales similarly over time. However,
 226 Thinking and HyT models achieve higher performance earlier and maintain higher success rate over
 227 time, compared to standard VLAs, which are between 5 and 20% less performant at any data scale.

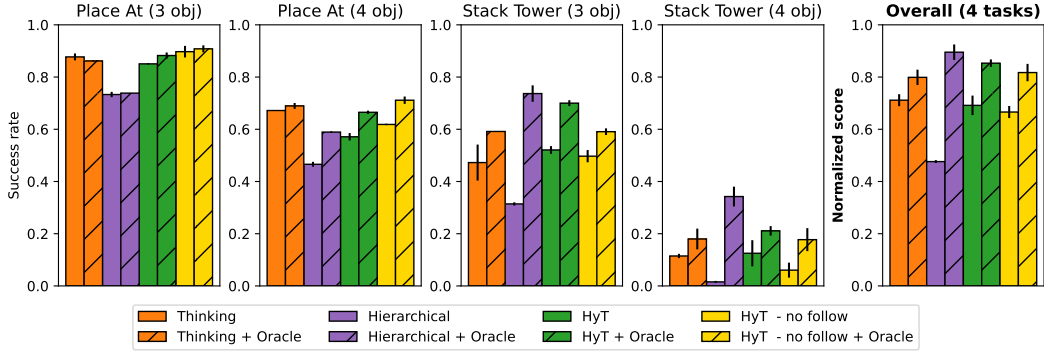


Figure 3: **Intervening on thoughts.** Comparing performance across thinking VLA, when using their own generated thoughts (default) or using thoughts generated by an oracle. Oracle thoughts are only provided for certain parts of tasks, i.e. the "move to X" subtasks. Actions are predicted by the VLA.

228 The fact that HyT - Fast is performing as well as Thinking and HyT - Slow VLAs confirm our
 229 hypothesis that directly predicting actions in Fast mode benefits from the hybrid thinking training.
 230 *Scale matters!* As a matter of fact, the performance increases with larger datasets across all tasks. The
 231 models saturate performance (close to 100%) on the easier tasks and start solving the most complex
 232 task, Stack Tower with 4 objects, at larger data scales.

233 Intervenability experiments

234 One useful feature of Thinking and Hierarchical models is the possibility to intervene on the model's
 235 thoughts. One way of intervening is to replace the agent's generated thoughts with human-determined
 236 thoughts to correct or steer the agent's behavior towards the solution of a task. Ideally, HyT models
 237 should also be intervenable. In particular, the addition of the "Follow" modality in Equation 3 should
 238 encourage the agents to condition its actions on the thoughts.

239 To verify this empirically, we train a set of models on a multitask dataset of 3000 demos.² At this
 240 data scale, the models should be able to easily solve easier tasks and have modest success on harder
 241 tasks. In order to improve success on harder tasks, we replace the agent's thoughts with a set of
 242 "Oracle thoughts", which we extract using the code from the ClevrSkills' oracle. Oracle thoughts
 243 replace the agent's thoughts only during moving subtasks, i.e. "move to location X". This is because
 244 the oracle has precise conditions for picking and placing. A learned policy not always satisfies them,
 245 while still being successful, causing the agent to get stuck.

246 We present results in Figure 3 for four of the most complex tasks of our benchmark. We also compare
 247 to an ablation of HyT that does not include the "Follow" component in Eq. 3, to verify whether
 248 the agent benefits or not from this component during training. We observe that overall all methods
 249 improve when provided oracle thoughts. In particular, hierarchical VLAs, which generally tend
 250 to perform worse than the other models, significantly improve in Stack tasks thanks to the oracle
 251 thoughts. Thinking and HyT VLAs receive similar improvements from using oracle thoughts,
 252 proving that HyT is definitely intervenable. HyT ablation performs slightly worse than its counterpart,
 253 showing a minor but still beneficial increase in performance when including the "Follow" modality
 254 during training, both with and without the oracle thoughts.

255 4.2 Real-world Experiments

256 One of the major benefits of the HyT approach is its capability to retain higher performance at a
 257 lower inference time, which is the same as with standard VLAs. This benefit mainly makes sense in
 258 real-world use-cases, where faster execution is important to carry out tasks quickly and to increase

²The choice of using a multitask dataset here is mostly to save compute. Hierarchical models, for instance, require training two models for each dataset. This is also the reason why we omitted them from the scaling experiments.

Table 1: Success rates on the real-world tasks and number of successful trials. Some pictures of the agent performing the tasks are available in Figure 1. Additional details are provided in Appendix.

	FT-OpenVLA	HyT- Fast
In-distribution tasks	52% (13/25)	72% (18/25)
Place the banana in the green bowl	70% (7/10)	70% (7/10)
Place the red cube in the brown bag	50% (3/6)	100% (6/6)
Place the tomato left of the lettuce	60% (3/5)	60% (3/5)
Place the zucchini in front of the green cube	0% (0/4)	50% (2/4)
Out-of-distribution tasks	29% (7/24)	54% (13/24)
Place the rubber duck in the green bowl	40% (4/10)	20% (2/10)
Place the mushroom in the brown bag	0% (0/6)	100% (6/6)
Place the purple die left of the lettuce	0% (0/4)	50% (2/4)
Place the zucchini in front of the red hexagon	75% (3/4)	75% (3/4)
Overall	41% (20/49)	63% (31/49)

259 the perceived quality of the agent’s execution. Thus, it is important to verify whether the findings in
 260 simulation about HyT transfer to real-world scenarios.

261 For our real-world experiments, we collected a dataset comprising 320 trajectories using a robotic
 262 setup featuring an UFactory xArm 6 with a flexible two-fingered gripper, operating on a white
 263 tabletop. The agent observes the environment through RGB images captured by a RealSense D435
 264 camera, positioned at a corner of the table. For the models, we start from the pre-trained OpenVLA
 265 model with 7B parameters [4] and compare directly to it. We perform LoRA fine-tuning with rank 32
 266 [41], a batch size of 8 and a learning rate of $5e - 4$, using the Adam optimizer [36].

267 Our evaluation spans two categories of tasks: in-distribution and out-of-distribution. The in-
 268 distribution set includes tasks for which the dataset contains at least 10 demonstrations. For the
 269 out-of-distribution set, we modify the in-distribution tasks by altering certain elements, such as
 270 the object to be picked or the reference object for placement, ensuring the agent encounters novel
 271 scenarios not present in the training data. See the Appendix for additional details.

272 The robot control frequency is ~ 3 Hz with no thinking and ~ 1 Hz with thinking. Thus, due to the
 273 long times required for thinking models evaluation, we study only the OpenVLA model fine-tuned
 274 on our dataset (using the original code) and HyT in Fast mode. The results, shown in Table 1, show
 275 that HyT overall significantly outperforms OpenVLA, especially in out-of-distribution tasks.

276 From a qualitative perspective, we notice that OpenVLA and HyT have similar flaws, e.g., they
 277 tend to pick objects with the wrong orientation. However, HyT tends to be more precise when
 278 reaching picking and placing positions, e.g. it never reached for the wrong object while OpenVLA
 279 did, eventually leading to a noticeable performance gap.

280 5 Conclusion

281 Thinking strategies for VLAs [8, 9] have shown important benefits in terms of performance and
 282 intervenability over standard VLAs, with the drawback of slower inference. In this work, we support
 283 the idea that the thinking process can be “internalized” by the model, developing some form of expert
 284 intuition [12]. We proposed the Hybrid Thinking framework that enables the agent to use different
 285 training and inference modalities. This enables the possibility of learning from thoughts, while also
 286 being able to predict actions directly. As empirically validated through simulated and real-world
 287 experiments, Hybrid Thinking VLAs can obtain data-efficient performance and intervenability, along
 288 with fast inference.

289 **Limitations.** Thoughts in robotics require an user to design a thought structure that is beneficial to the
 290 agent. Automated reasoning approaches to obtain useful thoughts may be explored [18]. In this work,
 291 we adopted large 3B and 7B parameters models. As we deploy faster models for computing actions
 292 on edge devices, we should aim to achieve similar performance with compute-efficient models [42].

293 **References**

294 [1] E. Collaboration, A. O'Neill, A. Rehman, A. Gupta, A. Maddukuri, A. Gupta, A. Padalkar, A. Lee,
 295 A. Pooley, A. Gupta, A. Mandlekar, A. Jain, A. Tung, A. Bewley, A. Herzog, A. Irpan, A. Khazatsky,
 296 A. Rai, A. Gupta, A. Wang, A. Kolobov, A. Singh, A. Garg, A. Kembhavi, A. Xie, A. Brohan, A. Raffin,
 297 A. Sharma, A. Yavary, A. Jain, A. Balakrishna, A. Wahid, B. Burgess-Limerick, B. Kim, B. Schölkopf,
 298 B. Wulfe, B. Ichter, C. Lu, C. Xu, C. Le, C. Finn, C. Wang, C. Xu, C. Chi, C. Huang, C. Chan, C. Agia,
 299 C. Pan, C. Fu, C. Devin, D. Xu, D. Morton, D. Driess, D. Chen, D. Pathak, D. Shah, D. Büchler,
 300 D. Jayaraman, D. Kalashnikov, D. Sadigh, E. Johns, E. Foster, F. Liu, F. Ceola, F. Xia, F. Zhao, F. V. Frujeri,
 301 F. Stulp, G. Zhou, G. S. Sukhatme, G. Salhotra, G. Yan, G. Feng, G. Schiavi, G. Berseth, G. Kahn, G. Yang,
 302 G. Wang, H. Su, H.-S. Fang, H. Shi, H. Bao, H. B. Amor, H. I. Christensen, H. Furuta, H. Bharadhwaj,
 303 H. Walke, H. Fang, H. Ha, I. Mordatch, I. Radosavovic, I. Leal, J. Liang, J. Abou-Chakra, J. Kim, J. Drake,
 304 J. Peters, J. Schneider, J. Hsu, J. Vakil, J. Bohg, J. Bingham, J. Wu, J. Gao, J. Hu, J. Wu, J. Wu, J. Sun,
 305 J. Luo, J. Gu, J. Tan, J. Oh, J. Wu, J. Lu, J. Yang, J. Malik, J. Silvério, J. Hejna, J. Booher, J. Tompson,
 306 J. Yang, J. Salvador, J. J. Lim, J. Han, K. Wang, K. Rao, K. Pertsch, K. Hausman, K. Go, K. Gopalakrishnan,
 307 K. Goldberg, K. Byrne, K. Oslund, K. Kawaharazuka, K. Black, K. Lin, K. Zhang, K. Ehsani, K. Lekkala,
 308 K. Ellis, K. Rana, K. Srinivasan, K. Fang, K. P. Singh, K.-H. Zeng, K. Hatch, K. Hsu, L. Itti, L. Y.
 309 Chen, L. Pinto, L. Fei-Fei, L. Tan, L. J. Fan, L. Ott, L. Lee, L. Weihs, M. Chen, M. Lepert, M. Memmel,
 310 M. Tomizuka, M. Itkina, M. G. Castro, M. Spero, M. Du, M. Ahn, M. C. Yip, M. Zhang, M. Ding, M. Heo,
 311 M. K. Srirama, M. Sharma, M. J. Kim, N. Kanazawa, N. Hansen, N. Heess, N. J. Joshi, N. Suenderhauf,
 312 N. Liu, N. D. Palo, N. M. M. Shafiuallah, O. Mees, O. Kroemer, O. Bastani, P. R. Sanketi, P. T. Miller, P. Yin,
 313 P. Wohlhart, P. Xu, P. D. Fagan, P. Mitrano, P. Sermanet, P. Abbeel, P. Sundareshan, Q. Chen, Q. Vuong,
 314 R. Rafailov, R. Tian, R. Doshi, R. Mart'in-Mart'in, R. Carbajal, R. Scalise, R. Hendrix, R. Lin, R. Qian,
 315 R. Zhang, R. Mendonca, R. Shah, R. Hoque, R. Julian, S. Bustamante, S. Kirmani, S. Levine, S. Lin,
 316 S. Moore, S. Bahl, S. Dass, S. Sonawani, S. Tulsiani, S. Song, S. Xu, S. Haldar, S. Karamcheti, S. Adebola,
 317 S. Guist, S. Nasiriany, S. Schaal, S. Welker, S. Tian, S. Ramamoorthy, S. Dasari, S. Belkhale, S. Park,
 318 S. Nair, S. Mirchandani, T. Osa, T. Gupta, T. Harada, T. Matsushima, T. Xiao, T. Kollar, T. Yu, T. Ding,
 319 T. Davchev, T. Z. Zhao, T. Armstrong, T. Darrell, T. Chung, V. Jain, V. Kumar, V. Vanhoucke, W. Zhan,
 320 W. Zhou, W. Burgard, X. Chen, X. Chen, X. Wang, X. Zhu, X. Geng, X. Liu, X. Liangwei, X. Li, Y. Pang,
 321 Y. Lu, Y. J. Ma, Y. Kim, Y. Chebotar, Y. Zhou, Y. Zhu, Y. Wu, Y. Xu, Y. Wang, Y. Bisk, Y. Dou, Y. Cho,
 322 Y. Lee, Y. Cui, Y. Cao, Y.-H. Wu, Y. Tang, Y. Zhu, Y. Zhang, Y. Jiang, Y. Li, Y. Li, Y. Iwasawa, Y. Matsuo,
 323 Z. Ma, Z. Xu, Z. J. Cui, Z. Zhang, Z. Fu, and Z. Lin. Open x-embodiment: Robotic learning datasets and
 324 rt-x models, 2024. URL <https://arxiv.org/abs/2310.08864>.

325 [2] A. Steiner, A. S. Pinto, M. Tschanne, D. Keysers, X. Wang, Y. Bitton, A. Gritsenko, M. Minderer,
 326 A. Sherbondy, S. Long, S. Qin, R. Ingle, E. Bugliarello, S. Kazemzadeh, T. Mesnard, I. Alabdulmohsin,
 327 L. Beyer, and X. Zhai. Paligemma 2: A family of versatile vlms for transfer, 2024. URL <https://arxiv.org/abs/2412.03555>.

328 [3] S. Tong, E. Brown, P. Wu, S. Woo, M. Middepogu, S. C. Akula, J. Yang, S. Yang, A. Iyer, X. Pan, Z. Wang,
 329 R. Fergus, Y. LeCun, and S. Xie. Cambrian-1: A fully open, vision-centric exploration of multimodal llms,
 330 2024. URL <https://arxiv.org/abs/2406.16860>.

331 [4] M. J. Kim, K. Pertsch, S. Karamcheti, T. Xiao, A. Balakrishna, S. Nair, R. Rafailov, E. Foster, G. Lam,
 332 P. Sanketi, et al. Openvla: An open-source vision-language-action model. *arXiv preprint arXiv:2406.09246*,
 333 2024.

334 [5] A. Brohan, N. Brown, J. Carbajal, Y. Chebotar, J. Dabis, C. Finn, K. Gopalakrishnan, K. Hausman,
 335 A. Herzog, J. Hsu, J. Ibarz, B. Ichter, A. Irpan, T. Jackson, S. Jesmonth, N. J. Joshi, R. Julian, D. Kalash-
 336 nikov, Y. Kuang, I. Leal, K.-H. Lee, S. Levine, Y. Lu, U. Malla, D. Manjunath, I. Mordatch, O. Nachum,
 337 C. Parada, J. Peralta, E. Perez, K. Pertsch, J. Quiambao, K. Rao, M. Ryoo, G. Salazar, P. Sanketi, K. Sayed,
 338 J. Singh, S. Sontakke, A. Stone, C. Tan, H. Tran, V. Vanhoucke, S. Vega, Q. Vuong, F. Xia, T. Xiao, P. Xu,
 339 S. Xu, T. Yu, and B. Zitzkovich. Rt-1: Robotics transformer for real-world control at scale, 2023. URL
 340 <https://arxiv.org/abs/2212.06817>.

341 [6] A. Brohan, N. Brown, J. Carbajal, Y. Chebotar, X. Chen, K. Choromanski, T. Ding, D. Driess, A. Dubey,
 342 C. Finn, P. Florence, C. Fu, M. G. Arenas, K. Gopalakrishnan, K. Han, K. Hausman, A. Herzog, J. Hsu,
 343 B. Ichter, A. Irpan, N. Joshi, R. Julian, D. Kalashnikov, Y. Kuang, I. Leal, L. Lee, T.-W. E. Lee, S. Levine,
 344 Y. Lu, H. Michalewski, I. Mordatch, K. Pertsch, K. Rao, K. Reymann, M. Ryoo, G. Salazar, P. Sanketi,
 345 P. Sermanet, J. Singh, A. Singh, R. Soricut, H. Tran, V. Vanhoucke, Q. Vuong, A. Wahid, S. Welker,
 346 P. Wohlhart, J. Wu, F. Xia, T. Xiao, P. Xu, S. Xu, T. Yu, and B. Zitzkovich. Rt-2: Vision-language-action
 347 models transfer web knowledge to robotic control, 2023. URL <https://arxiv.org/abs/2307.15818>.

348 [7] J. Wei, X. Wang, D. Schuurmans, M. Bosma, B. Ichter, F. Xia, E. Chi, Q. Le, and D. Zhou. Chain-of-
 349 thought prompting elicits reasoning in large language models, 2023. URL <https://arxiv.org/abs/2201.11903>.

350

351

352 [8] M. Zawalski, W. Chen, K. Pertsch, O. Mees, C. Finn, and S. Levine. Robotic control via embodied
353 chain-of-thought reasoning. *arXiv preprint arXiv:2407.08693*, 2024.

354 [9] L. X. Shi, B. Ichter, M. Equi, L. Ke, K. Pertsch, Q. Vuong, J. Tanner, A. Walling, H. Wang, N. Fusai,
355 A. Li-Bell, D. Driess, L. Groom, S. Levine, and C. Finn. Hi robot: Open-ended instruction following with
356 hierarchical vision-language-action models, 2025. URL <https://arxiv.org/abs/2502.19417>.

357 [10] NVIDIA, :, J. Bjorck, F. Castañeda, N. Cherniadev, X. Da, R. Ding, L. J. Fan, Y. Fang, D. Fox, F. Hu,
358 S. Huang, J. Jang, Z. Jiang, J. Kautz, K. Kundalia, L. Lao, Z. Li, Z. Lin, K. Lin, G. Liu, E. Llontop,
359 L. Magne, A. Mandlekar, A. Narayan, S. Nasiriany, S. Reed, Y. L. Tan, G. Wang, Z. Wang, J. Wang,
360 Q. Wang, J. Xiang, Y. Xie, Y. Xu, Z. Xu, S. Ye, Z. Yu, A. Zhang, H. Zhang, Y. Zhao, R. Zheng, and
361 Y. Zhu. Gr00t n1: An open foundation model for generalist humanoid robots, 2025. URL <https://arxiv.org/abs/2503.14734>.

363 [11] D. Kahneman. *Thinking, fast and slow*. macmillan, 2011.

364 [12] D. Kahneman and G. Klein. Conditions for intuitive expertise: a failure to disagree. *Am Psychol*, 64(6):
365 515–526, Sept. 2009.

366 [13] K. Black, N. Brown, D. Driess, A. Esmail, M. Equi, C. Finn, N. Fusai, L. Groom, K. Hausman, B. Ichter,
367 S. Jakubczak, T. Jones, L. Ke, S. Levine, A. Li-Bell, M. Mothukuri, S. Nair, K. Pertsch, L. X. Shi, J. Tanner,
368 Q. Vuong, A. Walling, H. Wang, and U. Zhilinsky. π_0 : A vision-language-action flow model for general
369 robot control, 2024. URL <https://arxiv.org/abs/2410.24164>.

370 [14] J. Wen, Y. Zhu, J. Li, M. Zhu, K. Wu, Z. Xu, N. Liu, R. Cheng, C. Shen, Y. Peng, F. Feng, and J. Tang.
371 Tinyvla: Towards fast, data-efficient vision-language-action models for robotic manipulation, 2024. URL
372 <https://arxiv.org/abs/2409.12514>.

373 [15] O. M. Team, D. Ghosh, H. Walke, K. Pertsch, K. Black, O. Mees, S. Dasari, J. Hejna, T. Kreiman, C. Xu,
374 J. Luo, Y. L. Tan, L. Y. Chen, P. Sanketi, Q. Vuong, T. Xiao, D. Sadigh, C. Finn, and S. Levine. Octo: An
375 open-source generalist robot policy, 2024. URL <https://arxiv.org/abs/2405.12213>.

376 [16] Y. Jiang, A. Gupta, Z. Zhang, G. Wang, Y. Dou, Y. Chen, L. Fei-Fei, A. Anandkumar, Y. Zhu, and L. Fan.
377 Vima: General robot manipulation with multimodal prompts, 2023. URL <https://arxiv.org/abs/2210.03094>.

378 [17] J. Wei, X. Wang, D. Schuurmans, M. Bosma, F. Xia, E. Chi, Q. V. Le, D. Zhou, et al. Chain-of-thought
379 prompting elicits reasoning in large language models. *Advances in neural information processing systems*,
380 35:24824–24837, 2022.

382 [18] DeepSeek-AI, D. Guo, D. Yang, H. Zhang, J. Song, R. Zhang, R. Xu, Q. Zhu, S. Ma, P. Wang, X. Bi,
383 X. Zhang, X. Yu, Y. Wu, Z. F. Wu, Z. Gou, Z. Shao, Z. Li, Z. Gao, A. Liu, B. Xue, B. Wang, B. Wu,
384 B. Feng, C. Lu, C. Zhao, C. Deng, C. Zhang, C. Ruan, D. Dai, D. Chen, D. Ji, E. Li, F. Lin, F. Dai, F. Luo,
385 G. Hao, G. Chen, G. Li, H. Zhang, H. Bao, H. Xu, H. Wang, H. Ding, H. Xin, H. Gao, H. Qu, H. Li, J. Guo,
386 J. Li, J. Wang, J. Chen, J. Yuan, J. Qiu, J. Li, J. L. Cai, J. Ni, J. Liang, J. Chen, K. Dong, K. Hu, K. Gao,
387 K. Guan, K. Huang, K. Yu, L. Wang, L. Zhang, L. Zhao, L. Wang, L. Zhang, L. Xu, L. Xia, M. Zhang,
388 M. Zhang, M. Tang, M. Li, M. Wang, M. Li, N. Tian, P. Huang, P. Zhang, Q. Wang, Q. Chen, Q. Du, R. Ge,
389 R. Zhang, R. Pan, R. Wang, R. J. Chen, R. L. Jin, R. Chen, S. Lu, S. Zhou, S. Chen, S. Ye, S. Wang, S. Yu,
390 S. Zhou, S. Pan, S. S. Li, S. Zhou, S. Wu, S. Ye, T. Yun, T. Pei, T. Sun, T. Wang, W. Zeng, W. Zhao, W. Liu,
391 W. Liang, W. Gao, W. Yu, W. Zhang, W. L. Xiao, W. An, X. Liu, X. Wang, X. Chen, X. Nie, X. Cheng,
392 X. Liu, X. Xie, X. Liu, X. Yang, X. Li, X. Su, X. Lin, X. Q. Li, X. Jin, X. Shen, X. Chen, X. Sun, X. Wang,
393 X. Song, X. Zhou, X. Wang, X. Shan, Y. K. Li, Y. Q. Wang, Y. X. Wei, Y. Zhang, Y. Xu, Y. Li, Y. Zhao,
394 Y. Sun, Y. Wang, Y. Yu, Y. Zhang, Y. Shi, Y. Xiong, Y. He, Y. Piao, Y. Wang, Y. Tan, Y. Ma, Y. Liu, Y. Guo,
395 Y. Ou, Y. Wang, Y. Gong, Y. Zou, Y. He, Y. Xiong, Y. Luo, Y. You, Y. Liu, Y. Zhou, Y. X. Zhu, Y. Xu,
396 Y. Huang, Y. Li, Y. Zheng, Y. Zhu, Y. Ma, Y. Tang, Y. Zha, Y. Yan, Z. Z. Ren, Z. Ren, Z. Sha, Z. Fu, Z. Xu,
397 Z. Xie, Z. Zhang, Z. Hao, Z. Ma, Z. Yan, Z. Wu, Z. Gu, Z. Zhu, Z. Liu, Z. Li, Z. Xie, Z. Song, Z. Pan,
398 Z. Huang, Z. Xu, Z. Zhang, and Z. Zhang. Deepseek-r1: Incentivizing reasoning capability in llms via
399 reinforcement learning, 2025. URL <https://arxiv.org/abs/2501.12948>.

400 [19] A. Havrilla, Y. Du, S. C. Raparthy, C. Nalmpantis, J. Dwivedi-Yu, M. Zhuravinskyi, E. Hambro,
401 S. Sukhbaatar, and R. Raileanu. Teaching large language models to reason with reinforcement learning.
402 *arXiv preprint arXiv:2403.04642*, 2024.

403 [20] H. Shao, S. Qian, H. Xiao, G. Song, Z. Zong, L. Wang, Y. Liu, and H. Li. Visual cot: Advancing
404 multi-modal language models with a comprehensive dataset and benchmark for chain-of-thought reasoning,
405 2024. URL <https://arxiv.org/abs/2403.16999>.

406 [21] Q. Zhao, Y. Lu, M. J. Kim, Z. Fu, Z. Zhang, Y. Wu, Z. Li, Q. Ma, S. Han, C. Finn, A. Handa, M.-Y. Liu,
 407 D. Xiang, G. Wetzstein, and T.-Y. Lin. Cot-vla: Visual chain-of-thought reasoning for vision-language-
 408 action models, 2025. URL <https://arxiv.org/abs/2503.22020>.

409 [22] Y. Deng, Y. Choi, and S. Shieber. From explicit cot to implicit cot: Learning to internalize cot step by step,
 410 2024. URL <https://arxiv.org/abs/2405.14838>.

411 [23] P. Yu, J. Xu, J. Weston, and I. Kulikov. Distilling system 2 into system 1, 2024. URL <https://arxiv.org/abs/2407.06023>.

413 [24] D. Su, S. Sukhbaatar, M. Rabbat, Y. Tian, and Q. Zheng. Dualformer: Controllable fast and slow thinking
 414 by learning with randomized reasoning traces, 2025. URL <https://arxiv.org/abs/2410.09918>.

415 [25] M. Zhu, Y. Zhu, J. Li, J. Wen, Z. Xu, Z. Che, C. Shen, Y. Peng, D. Liu, F. Feng, and J. Tang. Language-
 416 conditioned robotic manipulation with fast and slow thinking, 2024. URL <https://arxiv.org/abs/2401.04181>.

418 [26] A. Vaswani, N. Shazeer, N. Parmar, J. Uszkoreit, L. Jones, A. N. Gomez, L. Kaiser, and I. Polosukhin.
 419 Attention is all you need, 2023. URL <https://arxiv.org/abs/1706.03762>.

420 [27] T. B. Brown, B. Mann, N. Ryder, M. Subbiah, J. Kaplan, P. Dhariwal, A. Neelakantan, P. Shyam, G. Sastry,
 421 A. Askell, S. Agarwal, A. Herbert-Voss, G. Krueger, T. Henighan, R. Child, A. Ramesh, D. M. Ziegler,
 422 J. Wu, C. Winter, C. Hesse, M. Chen, E. Sigler, M. Litwin, S. Gray, B. Chess, J. Clark, C. Berner,
 423 S. McCandlish, A. Radford, I. Sutskever, and D. Amodei. Language models are few-shot learners, 2020.
 424 URL <https://arxiv.org/abs/2005.14165>.

425 [28] G. Team, M. Riviere, S. Pathak, P. G. Sessa, C. Hardin, S. Bhupatiraju, L. Hussenot, T. Mesnard,
 426 B. Shahriari, A. Ramé, J. Ferret, P. Liu, P. Tafti, A. Friesen, M. Casbon, S. Ramos, R. Kumar, C. L. Lan,
 427 S. Jerome, A. Tsitsulin, N. Vieillard, P. Stanczyk, S. Girgin, N. Momchev, M. Hoffman, S. Thakoor,
 428 J.-B. Grill, B. Neyshabur, O. Bachem, A. Walton, A. Severyn, A. Parrish, A. Ahmad, A. Hutchison,
 429 A. Abdagic, A. Carl, A. Shen, A. Brock, A. Coenen, A. Laforge, A. Paterson, B. Bastian, B. Piot, B. Wu,
 430 B. Royal, C. Chen, C. Kumar, C. Perry, C. Welty, C. A. Choquette-Choo, D. Sinopalnikov, D. Weinberger,
 431 D. Vijaykumar, D. Rogozińska, D. Herbison, E. Bandy, E. Wang, E. Noland, E. Moreira, E. Senter,
 432 E. Eltyshev, F. Visin, G. Rasskin, G. Wei, G. Cameron, G. Martins, H. Hashemi, H. Klimczak-Plucińska,
 433 H. Batra, H. Dhand, I. Nardini, J. Mein, J. Zhou, J. Svensson, J. Stanway, J. Chan, J. P. Zhou, J. Carrasqueira,
 434 J. Iljazi, J. Becker, J. Fernandez, J. van Amersfoort, J. Gordon, J. Lipschultz, J. Newlan, J. yeong Ji,
 435 K. Mohamed, K. Badola, K. Black, K. Millican, K. McDonell, K. Nguyen, K. Sodhia, K. Greene, L. L.
 436 Sjoesund, L. Usui, L. Sifre, L. Heuermann, L. Lago, L. McNealus, L. B. Soares, L. Kilpatrick, L. Dixon,
 437 L. Martins, M. Reid, M. Singh, M. Iverson, M. Görner, M. Veloso, M. Wirth, M. Davidow, M. Miller,
 438 M. Rahtz, M. Watson, M. Risdal, M. Kazemi, M. Moynihan, M. Zhang, M. Kahng, M. Park, M. Rahman,
 439 M. Khatwani, N. Dao, N. Bardoliwalla, N. Devanathan, N. Dumai, N. Chauhan, O. Wahltinez, P. Botarda,
 440 P. Barnes, P. Barham, P. Michel, P. Jin, P. Georgiev, P. Culliton, P. Kuppala, R. Comanescu, R. Merhej,
 441 R. Jana, R. A. Rokni, R. Agarwal, R. Mullins, S. Saadat, S. M. Carthy, S. Cogan, S. Perrin, S. M. R. Arnold,
 442 S. Krause, S. Dai, S. Garg, S. Sheth, S. Ronstrom, S. Chan, T. Jordan, T. Yu, T. Eccles, T. Hennigan,
 443 T. Kociský, T. Doshi, V. Jain, V. Yadav, V. Meshram, V. Dharmadhikari, W. Barkley, W. Wei, W. Ye,
 444 W. Han, W. Kwon, X. Xu, Z. Shen, Z. Gong, Z. Wei, V. Cotruta, P. Kirk, A. Rao, M. Giang, L. Peran,
 445 T. Warkentin, E. Collins, J. Barral, Z. Ghahramani, R. Hadsell, D. Sculley, J. Banks, A. Dragan, S. Petrov,
 446 O. Vinyals, J. Dean, D. Hassabis, K. Kavukcuoglu, C. Farabet, E. Buchatskaya, S. Borgeaud, N. Fiedel,
 447 A. Joulin, K. Kenealy, R. Dadashi, and A. Andreev. Gemma 2: Improving open language models at a
 448 practical size, 2024. URL <https://arxiv.org/abs/2408.00118>.

449 [29] A. Dosovitskiy, L. Beyer, A. Kolesnikov, D. Weissenborn, X. Zhai, T. Unterthiner, M. Dehghani, M. Min-
 450 derer, G. Heigold, S. Gelly, J. Uszkoreit, and N. Houlsby. An image is worth 16x16 words: Transformers
 451 for image recognition at scale, 2021. URL <https://arxiv.org/abs/2010.11929>.

452 [30] A. Paszke, S. Gross, S. Chintala, G. Chanan, E. Yang, Z. DeVito, Z. Lin, A. Desmaison, L. Antiga, and
 453 A. Lerer. Automatic differentiation in pytorch. 2017.

454 [31] S. Haresh, D. Dijkman, A. Bhattacharyya, and R. Memisevic. Clevrskills: Compositional language and
 455 visual reasoning in robotics, 2024. URL <https://arxiv.org/abs/2411.09052>.

456 [32] J. Gu, F. Xiang, X. Li, Z. Ling, X. Liu, T. Mu, Y. Tang, S. Tao, X. Wei, Y. Yao, X. Yuan, P. Xie, Z. Huang,
 457 R. Chen, and H. Su. Maniskill2: A unified benchmark for generalizable manipulation skills, 2023. URL
 458 <https://arxiv.org/abs/2302.04659>.

459 [33] C. Chi, Z. Xu, S. Feng, E. Cousineau, Y. Du, B. Burchfiel, R. Tedrake, and S. Song. Diffusion policy:
 460 Visuomotor policy learning via action diffusion, 2024. URL <https://arxiv.org/abs/2303.04137>.

461 [34] T. Z. Zhao, V. Kumar, S. Levine, and C. Finn. Learning fine-grained bimanual manipulation with low-cost
462 hardware, 2023. URL <https://arxiv.org/abs/2304.13705>.

463 [35] X. Zhai, B. Mustafa, A. Kolesnikov, and L. Beyer. Sigmoid loss for language image pre-training, 2023.
464 URL <https://arxiv.org/abs/2303.15343>.

465 [36] D. P. Kingma and J. Ba. Adam: A method for stochastic optimization, 2017. URL <https://arxiv.org/abs/1412.6980>.

466

467 [37] R. Sutton. The bitter lesson. *Incomplete Ideas (blog)*, 13(1):38, 2019.

468 [38] J. Fan. A review for deep reinforcement learning in atari:benchmarks, challenges, and solutions, 2023.
469 URL <https://arxiv.org/abs/2112.04145>.

470 [39] P. Mazzaglia, T. Verbelen, B. Dhoedt, A. Courville, and S. Rajeswar. Genrl: Multimodal-foundation world
471 models for generalization in embodied agents, 2024. URL <https://arxiv.org/abs/2406.18043>.

472 [40] N. Hansen, H. Su, and X. Wang. Td-mpc2: Scalable, robust world models for continuous control, 2024.
473 URL <https://arxiv.org/abs/2310.16828>.

474 [41] E. J. Hu, Y. Shen, P. Wallis, Z. Allen-Zhu, Y. Li, S. Wang, L. Wang, and W. Chen. Lora: Low-rank
475 adaptation of large language models, 2021. URL <https://arxiv.org/abs/2106.09685>.

476 [42] T. Dao and A. Gu. Transformers are ssms: Generalized models and efficient algorithms through structured
477 state space duality, 2024. URL <https://arxiv.org/abs/2405.21060>.

478 [43] R. Agarwal, M. Schwarzer, P. S. Castro, A. Courville, and M. G. Bellemare. Deep reinforcement learning
479 at the edge of the statistical precipice. *Advances in Neural Information Processing Systems*, 2021.

480 **A Appendix**

481 **A.1 Details about Figure 1**

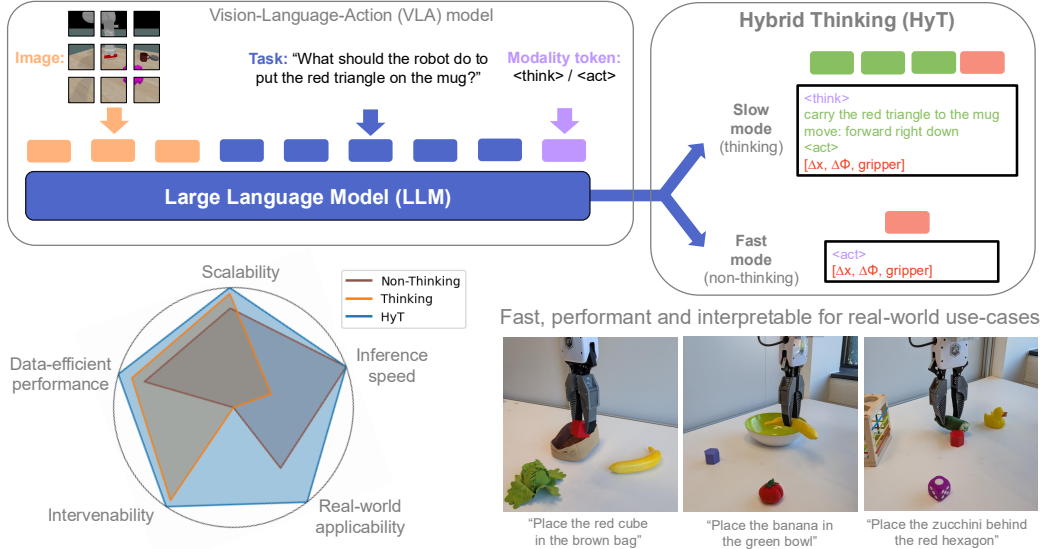


Figure 4: **Hybrid Thinking VLAs.** The hybrid thinking framework enables vision-language-action models to switch between fast execution and thoughtful - slow - execution. In addition to an image of the scene and a language description of the task, the agent receives a modality token, which conditions the output of the model. We observed that, even in the fast mode (high inference speed), the model has high performance, both in low-data (data-efficiency) and large-data (scalability) regimes. The high performance and fast inference speed enable fast and performant deployment in real-world scenarios (real-world applicability). The improved performance obtained when using ‘oracle’ thoughts together with the slow mode of HyT demonstrate the agent’s interpretability and the possibility to intervene on the thoughts for behavior’s correction (intervenability).

482 In the caption of Figure 4, we provide a detailed explanation of the HyT framework and performance.
 483 The radar plot in the Figure illustrates the results of standard VLAs as ‘Non-thinking’, thinking VLA
 484 as ‘Thinking’, and HyT. The data used for the radar plot is presented in Table 2 and obtained as
 485 follows:

- 486 • **Inference speed:** measured on (fractions of) A100 GPUs, while performing inference on
 487 the ClevrSkills tasks. HyT is in Fast mode;
- 488 • **Scalability:** overall normalized scores after training on the 4000 trajectories datasets on
 489 ClevrSkills (as in Figure 2). HyT results are obtained in Fast mode;
- 490 • **Data-efficient:** overall normalized scores after training on the 1500 trajectories multitask
 491 dataset and evaluating on ClevrSkills (see Table ??). HyT results are obtained in Fast mode;
- 492 • **Intervenability:** overall normalized scores when intervening on the thoughts (see Fig 3).
 493 HyT results must be obtained in Slow mode. Non-thinking is ‘NA’ as it doesn’t allow
 494 interventions on the thoughts;
- 495 • **Real-world:** overall success rate in real-world tasks (see Table 1). HyT results are obtained
 496 in Fast mode. Thinking VLAs are excluded from the comparison due to time constraints
 497 (the inference process is 3× slower).

Table 2: Max scores for different systems across evaluation dimensions

	Inference speed	Scalability	Data-efficient	Intervenability	Real-world
Non-thinking	3 Hz	0.76	0.33	NA	0.41
Thinking	1 Hz	0.88	0.37	0.80	NA
HyT	3 Hz	0.92	0.42	0.85	0.64

498 **A.2 Simulation experiments**

499 **Tasks definition** The tasks are defined as follows:

500 • *Place At* tasks evaluate the agent’s spatial understanding. The tasks require the agent to bring an
501 object to a location specified in relation to another object location, i.e. left/right/behind/in front of
502 the object. The objects used are mainly simple-shaped objects of different colors as in [16].
503 • *Place OnTop* tasks evaluate the agent’s understanding of object interactions, as they require placing
504 an object on top of another in a stable position. The set of objects used contains simple shapes, but
505 also more complex objects from YCB, such as mugs, wooden blocks, bowls, etc.
506 • *Stack Tower* evaluates the long-horizon capabilities of the agent, as it requires multiple “place on
507 top” with simple object shapes, where the order of the objects in the stack is defined in the prompt.

508 For each task, we train and test the agent with three variants, containing varying number of objects.
509 In *Place OnTop* and *Place At* the number of additional objects is only distracting or increasing the
510 amount of clutter in the scene, e.g. making placing objects on the table harder. For the *Stack Tower*
511 tasks more objects also require more actions, as the agent should stack all the objects present in the
512 scene.

513 **Evaluation details** At each episode, objects and positions are resampled randomly (but consistently
514 among evaluation runs), making no evaluation environment exactly the same as any of the training
515 examples. The agent is, thus, required to generalize actions to new settings in order to succeed. For
516 each model, we evaluate 3 checkpoints taken at epochs 5,7 and 10 during training. In general, we
517 found no strong correlation between validation losses and performance on the task. Though, with
518 additional training after 10 epochs, models tend to start overfitting.

519 **Dataset definition.** For each task group, we collected a set of 4000 demo trajectories composed as
520 follows: 1000 demos in the 2 objects task, 2000 demos in the 3 objects task, 1000 demos in the 4
521 objects task. Then, to train agents with different sizes of the dataset, we subsample fixed subsets of
522 trajectories from each dataset. For the multitask dataset, the task group datasets are subsampled and
523 then aggregated.

524 *Example 1: ‘Stack Tower’ task group dataset with 1000 demos (scaling experiments).* The 4000
525 demos dataset is subsampled, maintaining an equal ratio of trajectories per task. The number of
526 trajectories per task will be: 250 demos in the Stack Tower with 2 objects task, 500 demos in the
527 Stack Tower with 3 objects task, 250 demos in the Stack Tower with 4 objects task.

528 *Example 2: multitask dataset with 3000 demos (intervenability experiments).* For each task group, we
529 subsample a dataset of 1000 demos (see Example 1). Then, 3000 demos are obtained by aggregating
530 all the task groups’ demos.

531 **Extracting thoughts.** In ClevrSkills’ demonstrations [31] a variety of solvers is applied to the task,
532 following a pre-specified order - the oracle’s plan. Each solver takes executes one subtask from
533 the overall plan and the solver parameters can be recovered in the demonstrations. In order to create
534 thoughts, we can use the ClevrSkills library to transform each subtask from the solver into a natural
535 language instruction, e.g. “Move to X” or “Pick up Y”. Then, for moving instructions - e.g. “Move
536 to...” and “Carry Z to...” - we extract the motion direction of the agent. Similarly to [9], this is
537 obtained at each timestep by computing the distance between the current end-effector position and
538 the position at the end of the motion subtask. This is then transformed into language, in the form
539 of “left/right”, “forward/backward” and “up/down” instructions, as in [8]. Finally, for distances that
540 are less than 1 cm the agent receives a “close” moving instruction. Two examples of thoughts and
541 actions, in the HyT format, are provided in Figure 5.

542 **Gripper information.** The ClevrSkills benchmark adopts a vacuum-gripper robot which creates a
543 vacuum in the gripper’s suction cups to maintain contact with objects. Compared to a fingers-based
544 gripper, a suction gripper’s state, i.e. open or closed, cannot be easily assessed through images. Thus,
545 in order for the agent to be able to perform grasping actions reliably, we concatenate the state of the
546 gripper in language form to the task description (or to the thoughts for the hierarchical low-level
547 VLA). The gripper state information we pass to the agent is: (i) whether the gripper suction cups are
548 making contact with something, (ii) whether the gripper was on, grasping something, or not. There’s
549 no need for the gripper information in the real-world experiments, as we use a fingers-based gripper,
550 where the gripper state is visually observable.

<think>
 carry the red triangle to the mug
 move: forward right down
<act>
 $[\Delta x, \Delta \phi, \text{gripper}]$

(a)

<think>
 pick up the red triangle
<act>
 $[\Delta x, \Delta \phi, \text{gripper}]$

(b)

Figure 5: Examples of thoughts and actions for a moving (a) and a non-moving (b) subtasks, expressed in language format following the format used for HyT.

551 A.3 Normalizing scores

552 In Figures 1 and 3 we used ‘normalized scores’ to provide aggregate results across different tasks. This
 553 is typically done when different tasks have results in different scales across a benchmark [40, 39, 38].
 554 In Table 3, we report the highest success rates obtained by any approach in each task. We see that
 555 for some tasks the success rate is significantly lower than for others, e.g. Stack Tower with 3 and 4
 556 objects and Place At with 4 objects are harder to solve. Thus, when showing ‘overall’ performance,
 557 we rescale the results on each task in [0,1] by dividing them by the maximum obtained in that task -
 558 that is shown in the Table. Then, results are aggregated into ‘normalized scores’ providing a more
 559 insightful view on each approach’s relative performance [43].

Table 3: Highest success rate obtained by any approach (at any scale) and used to normalize scores.

Category	2 Objects	3 Objects	4 Objects
Place At	0.96	0.91	0.71
Place OnTop	0.84	0.80	0.80
Stack Tower	0.99	0.79	0.34

560 A.4 Real-world experiments



Figure 6: The setup for some of the real-world tasks: (a) banana in green bowl (b) red cube in brown bag (c) zucchini in front of green cube (d) tomato left of lettuce.

561 **Dataset preparation.** The dataset for real-world experiments is collected via human tele-operation,
 562 using a VR set and a controller to map the human motions and intentions, e.g., closing the gripper, to
 563 the robot. After collecting the trajectories, we apply some basic pre-processing operations. First, we
 564 take the sequences collected at 60 Hz, and we subsample them at 10 Hz. Then, we extract actions
 565 in the format $[\Delta x, \Delta \phi, \text{gripper}]$ from the end-effector and gripper positions of the demonstrations.
 566 Finally, we filter out no-motion operations, i.e. having Δx and $\Delta \theta$ equal to zero.

567 **Extracting thoughts.** For extracting the subtasks to use in the thoughts, we use a simple heuristic-
 568 based approach. This is based on the assumption that all the tasks in the dataset are in the format
 569 ‘place the {obj1} {position} the {obj2}’, e.g. ‘place the {zucchini} {in front of} the {green cube}’.
 570 We identify the position when the robot closes the gripper as the *grasping position*, and the position
 571 when the robot opens the gripper as the *releasing position*. Then, we identify the following 3 keyframe
 572 moments: (i) the moment when the agent reaches within 3 cms distance from the grasping position,

573 (ii) the grasping moment, (iii) the moment when the agent reaches within 3 cms distance from the
574 releasing position. Finally, the subtasks are defined in the trajectory as follows:

575 • *Move to the {obj1}*: between the start of the trajectory and keyframe (i);
576 • *Pick up the {obj1}*: between keyframe (i) and keyframe (ii);
577 • *Move {position} the {obj2}*: between keyframe (ii) and keyframe (iii);
578 • *Place object {position} the {obj2}*: between keyframe (iii) and the end of the trajectory.

579 Also, to have the same thought structure as in the ClevrSkills’ experiments, we concatenate a ‘move:
580 {direction}’ to the moving subtasks, where the direction is computed using the end-effector position
581 (see Section A.2).

582 **Evaluation.** During evaluation, we limit the execution time to 150 agent steps, which is ~ 2 minutes
583 per trajectory, considering 3 actions/second from the model and a control loop running at ~ 2 Hz for
584 stable motions. In case of failed grasps, we allow up to 3 attempts to the agent, before assessing the
585 outcome of the episode. In the following, you find a detailed description of how each in-distribution
586 task is executed and randomized. For out-of-distribution tasks, we follow the same procedures, but
587 we swap one of the main actors in the scene (e.g. the object to pick or the placing target). See Figure
588 6) for reference. Note: fruits are stuffed toys, while vegetables are hard foam models.

589 • *Place the banana in the green bowl*. The scene includes a green bowl and three objects: a
590 banana, a tomato, and a blue hexagon, each with predefined positions. We conduct five trials
591 with the banana starting in one location, and five more from a different location. In each
592 location, the banana appears in three orientations: vertical (2/5 trials), horizontal (2/5 trials),
593 and diagonal (1/5 trial).
594 • *Place the red cube in the brown bag*. The setup features a brown bag and three objects: a
595 red cube, a banana, and a lettuce leaf, all placed at specific locations. We run two trials for
596 each location of the red cube. Its orientation varies between being aligned with the robot’s
597 base and being tilted.
598 • *Place the tomato left of the lettuce*. The scene contains three objects: a lettuce leaf, a carrot,
599 and a tomato. Their positions are randomized within defined regions, though the overall
600 layout remains consistent. We perform five trials with these randomized placements. A trial
601 is only considered successful if the tomato ends up on the table, near the lettuce, and to its
602 left.
603 • *Place the zucchini in front of the green cube*. The environment includes five objects: a shape
604 sorting box, a zucchini, a purple die, a rubber duck, and a green cube. Object positions are
605 randomized within certain bounds, while maintaining the general layout. We carry out four
606 trials with these randomized setups. Success is defined as the zucchini being placed on the
607 table, close to and in front of the green cube.